AIP | The Journal of Chemical Physics

Hydrogen activation, diffusion, and clustering on CeO2(111): A DFT+U study

Delia Fernández-Torre, Javier Carrasco, M. Verónica Ganduglia-Pirovano, and Rubén Pérez

Citation: The Journal of Chemical Physics **141**, 014703 (2014); doi: 10.1063/1.4885546

View online: http://dx.doi.org/10.1063/1.4885546

View Table of Contents: http://scitation.aip.org/content/aip/journal/jcp/141/1?ver=pdfcov

Published by the AIP Publishing

Hydrogen activation, diffusion, and clustering on CeO_2(111): A DFT+*U* study

Delia Fernández-Torre,[1,2] Javier Carrasco,[3,4] M. Verónica Ganduglia-Pirovano,[4] and Rubén Pérez[1,5,a)]

[1]*Departamento de Física Teórica de la Materia Condensada, Universidad Autónoma de Madrid, E-28049 Madrid, Spain*
[2]*Instituto de Estructura de la Materia, CSIC, C/ Serrano 121, E-28006 Madrid, Spain*
[3]*CIC Energigune, Albert Einstein 48, 01510 Miñano, Álava, Spain*
[4]*Instituto de Catálisis y Petroleoquímica, CSIC, C/ Marie Curie 2, E-28049 Madrid, Spain*
[5]*Condensed Matter Physics Center (IFIMAC), Universidad Autónoma de Madrid, E-28049 Madrid, Spain*

(Received 19 May 2014; accepted 16 June 2014; published online 2 July 2014)

We present a comprehensive density functional theory+*U* study of the mechanisms underlying the dissociation of molecular hydrogen, and diffusion and clustering of the resulting atomic species on the CeO_2(111) surface. Contrary to a widely held view based solely on a previous theoretical prediction, our results show conclusively that H_2 dissociation is an activated process with a large energy barrier ∼1.0 eV that is not significantly affected by coverage or the presence of surface oxygen vacancies. The reaction proceeds through a local energy minimum – where the molecule is located close to one of the surface oxygen atoms and the H–H bond has been substantially weaken by the interaction with the substrate –, and a transition state where one H atom is attached to a surface O atom and the other H atom sits on-top of a Ce^{4+} ion. In addition, we have explored how several factors, including H coverage, the location of Ce^{3+} ions as well as the *U* value, may affect the chemisorption energy and the relative stability of isolated OH groups versus pair and trimer structures. The trimer stability at low H coverages and the larger upward relaxation of the surface O atoms within the OH groups are consistent with the assignment of the frequent experimental observation by non-contact atomic force and scanning tunneling microscopies of bright protrusions on three neighboring surface O atoms to a triple OH group. The diffusion path of isolated H atoms on the surface goes through the adsorption on-top of an oxygen in the third atomic layer with a large energy barrier of ∼1.8 eV. Overall, the large energy barriers for both, molecular dissociation and atomic diffusion, are consistent with the high activity and selectivity found recently in the partial hydrogenation of acetylene catalyzed by ceria at high H_2/C_2H_2 ratios. © *2014 AIP Publishing LLC*. [http://dx.doi.org/10.1063/1.4885546]

I. INTRODUCTION

Ceria (CeO_2) is a technologically important material with applications in fields as diverse as catalysis,[1] solid-oxide fuel cells,[2] and biomedicine.[3] Most applications of CeO_2 are linked to its redox properties, which include easy uptake, release, and diffusion of oxygen. The basic process underlying the redox chemistry of CeO_2 is the facile change in the oxidation state of the cerium ions ($Ce^{4+} \leftrightarrow Ce^{3+}$). In catalysis, ceria acts typically as an active support by providing lattice oxygen atoms when required. For instance, the active role of ceria in the catalysis of metal/ceria systems for the water-gas shift reaction,[4,5] and the preferential oxidation of CO,[6] has been widely reported. However, oxygen is not the only relevant species in the chemistry promoted by ceria. Surface hydroxyls are very common on ceria surfaces and are involved as surface intermediates in all of these important reactions.

The interaction of H_2 with ceria by temperature programmed reduction (TPR) has been widely used to obtain information on the system reducibility.[7,8] Ceria can be reduced by H_2 at temperatures higher than 600 K, and its reduction is strongly affected by textural and morphological properties. The process is generally thought to start with the hydroxylation of the surface—with concomitant reduction of Ce^{4+} to Ce^{3+}, and then to proceed with the incorporation of hydrogen in the bulk. Furthermore, hydroxylated ceria surfaces have been created by exposure to atomic H[9] and H_2O,[7,9–23] with the presence of oxygen vacancies being responsible for the dissociation of water. Such hydroxylated surfaces have been characterized by high-resolution imaging studies using non-contact Atomic Force (nc-AFM)[13] and Scanning Tunneling (STM) microscopy[19] with the focus on the most stable CeO_2(111) surface. Bright spots, commonly associated with hydroxyl groups on-top of a surface O atom, O_{surf}, were observed to form a triangular-shaped defect centered on an O atom in the third atomic layer, O_{sub}. In fact, such trimers are the most frequently observed OH species. Ceria has been applied in the formulation of various alkyne and alkadiene hydrogenation catalysts, acting as a promoter or stabilizer and, most commonly, as a carrier of noble metal nanoparticles.[24–26] However, recently, a stand-alone function in hydrogenation catalysis has been reported.[27] Ceria exhibits

a)ruben.perez@uam.es

a high-conversion rate and a remarkable selectivity in the partial gas-phase hydrogenation of alkynes. With a propene selectivity of 91% at ca. 100% propyne conversion,[27] ceria is one of the most effective catalysts ever reported for this family of reactions. In contrast, other reducible oxides such as TiO_2 and ZnO are inactive under similar conditions. The high temperature and the large H_2/alkyne ratio required to achieve the maximum conversion efficiency (e.g., 473 K and a 30:1 ratio for acetylene) suggest that H_2 dissociation is the rate-limiting step in the conversion of alkynes to olefins.[27]

Numerous density functional theory (DFT) based studies have addressed the interaction of water with clean and reduced ceria surfaces.[18,21,28–35] For CeO_2(111), there is agreement that isolated water molecules (i) adsorb on top of a Ce^{4+} atom, (ii) can be found in either a molecular state or as a hydroxyl pair,[32–35] and (iii) dissociate effectively barrierless on surface O vacancies.[29,32] The interaction of hydrogen with CeO_2(111) has also been intensively investigated,[20,22,23,28–30,32,36–38] with the molecular dissociation having received notoriously less attention.[28,32] The dissociative hydrogen adsorption reaction producing hydroxylated surfaces is exothermic within the 0.4–1.4 eV per $\frac{1}{2}H_2$ range. Quantitative discrepancies are due to the different DFT-based approaches DFT with the generalized gradient approximation (GGA) and DFT+U (U is a Hubbard-like term describing the onsite Coulomb interactions)] adopted in these works, and to the different hydrogen coverages used in the simulations. For example, Chen *et al.*,[28] using the Perdew-Wang (PW91)[39] exchange-correlation (XC) functional, $U = 6.3$ eV, and a $(\sqrt{3} \times 1)$ surface unit cell, reported a 1.4 eV per $\frac{1}{2}H_2$ reaction energy. In addition, their calculations suggest that the activation barrier for the hydrogen dissociation leading to the hydroxylation of the surface is small (~0.2 eV). Marrocchelli *et al.*[32] did not investigate the H_2 dissociation reaction but the reaction mechanisms between the H_2S and H_2O molecules on the CeO_2(111), and reported a high-energy barrier (~2.2 eV) for the reverse reaction, that goes from the fully dissociated molecule (H + H + S) to the (H_2 + S) configuration, where an H_2 molecule has been formed from adsorbed H atoms on neighboring O sites. These calculations employed also a DFT+U approach but with the Perdew-Burke-Ernzerhof (PBE) exchange-correlation functional,[40] a $U = 5$ eV, and a $(\sqrt{3} \times 2)$ cell. We note that a small H_2 dissociation barrier is in fundamental conflict with the large temperatures needed for ceria reduction,[7,8] and the results of the alkyne hydrogenation catalyzed by ceria reported above, in particular, the high temperature and the large H_2/alkyne ratio required to achieve the maximum conversion efficiency.[27] Moreover, the presence of surface oxygen vacancies has a detrimental effect. Clearly, a review of the mechanism of the H_2 dissociation (activation) on the CeO_2(111) surface is necessary to achieve a consistent description of the hydrogen-ceria system.

In this work, using DFT(GGA)+U ($U = 4.5$ eV), we re-examine the H_2/CeO_2(111) system employing various surface unit cells, namely, $(\sqrt{3} \times 1)$, (2×2), (3×3), and (4×4), and considering different possible configurations for the adsorbate and the Ce^{3+} ions resulting from the hydroxylation, in order to address the H_2 adsorption and dissociation on the clean surface.

The larger unit cells make also possible the study of the stability of OH trimers – three OH groups forming a triangle centered on an O_{sub} atom in the third atomic layer –, in order to substantiate their identification as the triangular defects commonly observed in STM and AFM experiments. In addition, the possible influence of the exchange-correlation functional and the value of the U parameter has also been considered. We produce firm computational evidence that the barrier for H_2 dissociation on CeO_2(111) is of the order of 1 eV, significantly larger (by ~0.8 eV) than the value reported by Chen and co-workers.[28] Comparing our results with the above mentioned theoretical studies we are able to give a comprehensive view of the process and, to a certain extent, rationalize the discrepancies. Furthermore, using a (2×2) unit cell, the effect of the presence of surface oxygen vacancies has been investigated finding that the H_2 dissociation barrier remains about the same as for the clean surface. Finally, we also analyze the activation barrier for hydrogen diffusion, which has important implications in all of the chemical reactions on ceria where H is involved.[27,41]

II. COMPUTATIONAL DETAILS

All of the calculations have been performed using the spin-polarized DFT+U approach[42] with (mostly) the PBE functional[40] as implemented in the Vienna *ab initio* simulation package (VASP, version 5.2.12).[43,44] The spin and the Hubbard-like term (the difference between the Coulomb U and exchange J parameters from here below referred as U) were necessary to describe the localized Ce 4*f* states that appear when the surface is reduced by the presence of an oxygen vacancy or adsorbed H atoms. We used projector-augmented wave (PAW) potentials with Ce (5*s*, 5*p*, 6*s*, 4*f*, 5*d*) and O (2*s*, 2*p*) electrons included in the valence, and a plane-wave cutoff of 400 eV. Our chosen effective $U = 4.5$ eV value has been calculated self-consistently by Fabris *et al.*[45] using the linear response approach of Cococcioni and de Gironcoli[46] and is within the 3.0–5.5 eV range that provides localization of the electrons left upon oxygen removal from CeO_2.[47] We have also performed selected calculations using the Perdew-Wang (PW91)[39] functional with $U = 6.3$ eV in order to compare our results with those in Ref. 28. In addition, for H_2 molecular adsorption, we have also compared the PBE+U binding energy with that obtained by the non-local optB86b-vdW+U functional,[48] as implemented in VASP; it corresponds to a modified version of the non-local vdW-density functional by Dion *et al.*[49] The performance of different vdW-inclusive functionals is still to be fully assessed.[50,51] However, the optB86b-vdW functional provides a good agreement between experimental adsorption energies and geometries and calculated values for benzene on several transition metal surfaces, a system considered as a benchmark.[52–55] In the PW91+U and optB86b-vdW+U calculations, core electrons were replaced by PW91- and PBE-based PAW potentials, respectively.

The CeO_2 surface was modeled using a supercell containing a slab of six atomic layers (2 trilayers, 2TL) with calculated CeO_2 bulk equilibrium lattice constant (5.485 Å) out

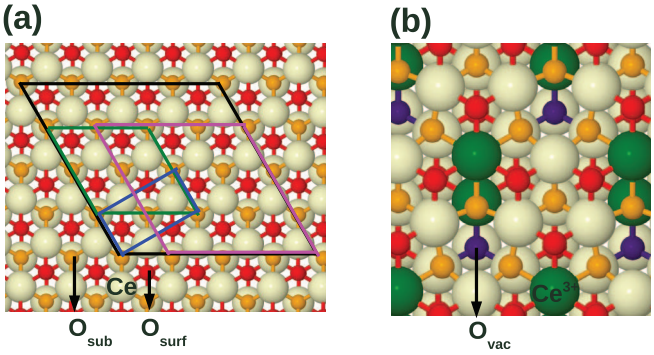

FIG. 1. Structural models. (a) Clean $CeO_2(111)$ surface (top view). Indicated are the (4×4), (3×3), (2×2), and ($\sqrt{3}$×1) surface unit cells in black, magenta, green, and blue, respectively. (b) Surface oxygen vacancy structure with (2×2) periodicity (top view). Oxygen atoms in the first (third) atomic layer, O_{surf} (O_{sub}), are red (orange), Ce^{4+} ions are pale yellow, Ce^{3+} ions are green, and the oxygen vacancy site is indigo.

of which three were allowed to relax with the surface unit cell kept fixed during geometry optimization. The vacuum layer was about 10 Å. We studied the H_2 dissociation on the clean (111) surface for varying coverage quantified with respect to the exposed cerium atoms, θ = 1/16, 1/9, 1/4, and 1/2 H_2 ML with a (4×4), (3×3), (2×2), and ($\sqrt{3}$×1) periodicity and a (2×2×1), (2×2×1), (3×3×1), and (6×6×1) Monkhorst-Pack grid, respectively. Selected calculations using thicker slabs have been performed with the smaller unit cells. In the (2×2) periodicity, results with 3TL (with the bottom TL fixed) did not change with respect to those for the thinner slab. In the case of the ($\sqrt{3}$×1) unit cells, we have performed calculations with 3 and 4 TL in order to rule out the influence of slab thickness in the fundamental discrepancies between our results and those of Ref. 28. The (3×3) cell has been considered for the study of the diffusion of atomic H. The structures were considered relaxed when all forces were smaller than 0.05 eV/Å and the convergence criterion for the energy was 10^{-4} eV.

We have also studied the dissociation of H_2 on a reduced $CeO_{2-x}(111)$ surface with surface oxygen vacancies. The defective structure was modeled using a supercell containing a slab of nine atomic layers and a (2×2) periodicity (i.e., 1/4 vacancies per surface unit cell). In this system, one Ce^{3+} ion is located in the second atomic layer and the other one in the fifth atomic layer (see Fig. 1(b)), according to the latest published results for the lowest energy configuration of the system with respect to the Ce^{3+} location upon creation of a surface vacancy.[56,57]

To locate the transition state structure for hydrogen dissociation we employed the climbing image nudged elastic band method (CI-NEB).[58] We characterized the transition structures by vibrational analysis. Harmonic vibrational frequencies and normal modes were obtained by diagonalizing the mass weighted force-constant matrix in Cartesian coordinates. A step of ±0.01 Å was set to calculate the force constants.

In the following, H_2 reaction (binding) energies are defined with respect to the total energy of the isolated H_2 molecule (or $\frac{1}{2}H_2$, for the case of atomic H) and the total energy of the clean (or reduced) $CeO_2(111)$ surface.

III. MOLECULAR ADSORPTION: H_2 ON $CeO_2(111)$

In a previous theoretical study[28] performed with the PW91+U (U = 6.3 eV) methodology using a ($\sqrt{3}$×1) surface unit cell, several weakly bonded adsorption structures were reported, and a configuration with H_2 adsorbed on-top of O_{surf} with the molecular axis perpendicular to the surface was found to be marginally more stable (by 0.01 eV) than others (see the top left panel of Fig. 2, structure labeled H_2–O_{surf}). Here we have considered the same system with PBE+U

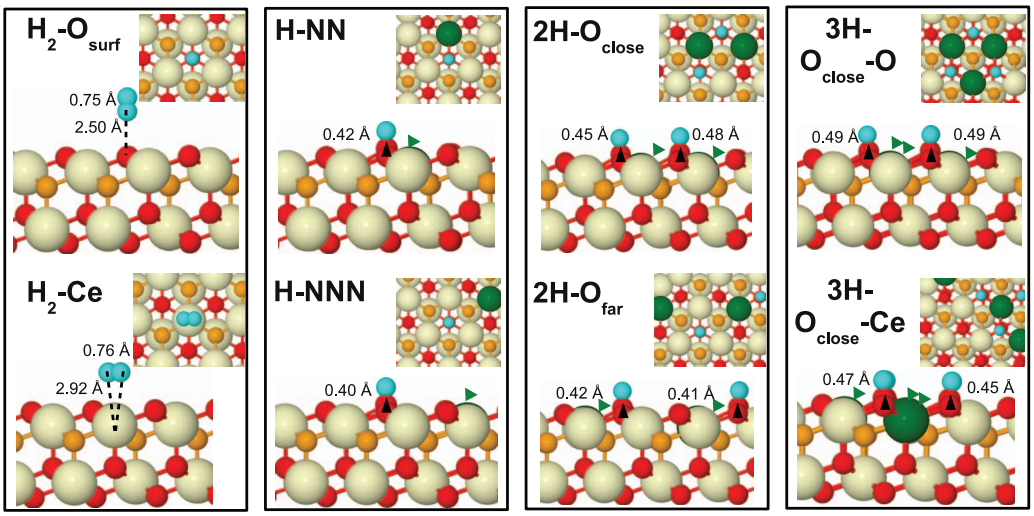

FIG. 2. Relevant structures for H_2 adsorption and dissociation on the clean $CeO_2(111)$ with a (4×4) periodicity. H_2–O_{surf}, H_2–Ce: physisorbed H_2; H-NN, H-NNN: chemisorbed H; 2H–O_{close}, 2H–O_{far}: two chemisorbed H atoms; 3H–O_{close}–O and 3H–O_{close}–Ce: three chemisorbed H atoms forming a triangle. The labels H-NN and H-NNN refer to the location of the Ce^{3+} ions in nearest or next-nearest neighboring cationic sites to the chemisorbed H on O_{surf}; 2H–O_{close} and 2H–O_{far} refer to the distance between O_{surf} atoms onto which H is chemisorbed (see text for details). The color code for the surface atoms is the same as in Fig. 1, with H atoms in cyan. Black triangles highlight atomic displacements and green triangles indicate the position of the Ce^{3+} ions. The numbers indicate interatomic Ce–H, O–H, and H–H distances for the molecular adsorption and the O_{surf} displacements for the H, 2H, and 3H structures.

TABLE I. Binding energies of H_2 (in eV/H_2), H and H pair, 2H (with respect to $\frac{1}{2}H_2$ in eV/H) adsorbed on clean CeO_2(111). The energy of the transition state structures (TS-diss) and the intermediate local energy minimum (LEM-diss) for the dissociation process on the (3×3), (2×2), and ($\sqrt{3}$×1) periodicities calculated in this work are referred to H_2–Ce, while the ($\sqrt{3}$×1) calculation by Chen *et al.* refers to their minimum, H_2–O_{surf}. All the adsorption structures specified in the table are shown in Fig. 2 for a (4×4) cell. 2TL models unless otherwise indicated.

Reference	Method	Unit cell	H_2–O_{surf}	H_2–Ce	H-NN	H-NNN	2H–O_{close}	TS-diss	LEM-diss
This work	optB86b-vdW+U(4.5 eV)	(4 × 4)	−0.07	−0.08	…	…	…	…	…
This work	PBE+U(4.5 eV)	(4 × 4)	−0.02	−0.03	−1.17	−1.16	−1.20[a]	…	…
Penschke *et al.*[59]	PBE+U(4.5 eV)[b,c]	(4 × 4)	…	…	…	−1.07	…	…	…
This work	PBE+U(4.5 eV)	(3 × 3)	−0.02	−0.03	−1.16	−1.17	−1.19	0.99	0.76
Popa *et al.*	PBE+U(4.5 eV)[c]	(3 × 3)	…	…	−1.17	−1.21	…	…	…
This work	PBE+U(4.5 eV)[c]	(2 × 2)	−0.02	−0.03	−1.14	−1.28	−1.17	0.99	0.77
Ganduglia-Pirovano *et al.*[60]	PBE+U(4.5 eV)[c]	(2 × 2)	…	…	…	−1.21	…	…	…
This work	PBE+U(4.5 eV)[c]	($\sqrt{3}$×1)	−0.02	−0.03	…	…	−1.15	1.00	0.85
Vicario *et al.*[37]	PBE+U(4 eV)[c]	($\sqrt{3}$×1)	…	…	−1.33	…	…	…	…
This work	PW91+U(6.3 eV)[c]	($\sqrt{3}$×1)	−0.03	−0.04	…	…	−1.60	0.85	0.84
This work	PW91+U(6.3 eV)[d]	($\sqrt{3}$×1)	…	…	…	…	−1.59	…	…
Chen *et al.*[28]	PW91+U(6.3 eV)[d]	($\sqrt{3}$×1)	−0.02	−0.01	…	…	−1.40	0.24	…

[a]The energy for the 2H–O_{far}, 3H–O_{close}–O, and 3H–O_{close}–Ce is, respectively, −1.20, −1.22, and −1.19 eV/H
[b]Using a plane-wave cutoff of 600 eV.
[c]Using 3 O–Ce–O trilayers (TL).
[d]Using 4 TL.

(U = 4.5 eV) at various coverages, namely, θ = 1/16, 1/9, 1/4, and 1/2 H_2 ML with a (4×4), (3×3), (2×2), and ($\sqrt{3}$×1) periodicity, respectively. Initially, we placed the H_2 molecule parallel and perpendicular to the surface over different sites: atop a first-layer oxygen, O_{surf}, a second-layer cerium, Ce, a third-layer oxygen, O_{sub} (Fig. 1(a)), and also on bridging positions.

We found two physisorption configurations, H_2–O_{surf} and H_2–Ce (Fig. 2), with binding energies of a few tens of meV (Table I) for all coverages investigated. Both structures were also reported in the previous work by Chen *et al.*,[28] but the relative stability was actually reversed with respect to our calculations. This discrepancy is clearly related to the XC functional and the U value as we did reproduce their results using their computational setup.

To estimate how important are the van der Waals interactions between molecule and surface, we have further relaxed the H_2–O_{surf} and H_2–Ce (4×4) structures with the optB86b-vdW+U functional. Using this method, the binding slightly increases (∼50 meV, see Table I) for both adsorption sites. This small energy increase is consistent with the low polarizability of the hydrogen molecule.

The binding energies for all H_2/CeO_2(111) structures considered in this work are very small and close to each other. A weak H_2–CeO_2(111) interaction implies a flat potential energy surface and, therefore, H_2 molecules can easily diffuse over the surface even at low temperatures.

IV. ATOMIC ADSORPTION: H, 2H, AND 3H ON CeO_2(111)

We have re-examined the adsorption energy of isolated H atoms and explored the relative stability of pairs and trimers using different unit cells. Pairs are relevant for the study of the molecular dissociation and trimers have been identified as common defects in nc-AFM and STM studies.

The adsorption of a single H atom has been already considered in the literature.[37,38,59] Our results confirm that adsorption on-top of O_{surf} is the lowest energy configuration, with the site on-top of O_{sub}) being 1.6 eV higher in energy on a (3×3) surface unit cell. This same value has been obtained in Ref. 37 using the PBE+U (U = 4 eV) methodology and a ($\sqrt{3}$×1) surface unit cell. Previous theoretical works have shown that when a single H atom is adsorbed on the clean CeO_2(111) surface, its electron is transferred to a 4*f* state of a cerium ion, nominally reducing it from Ce^{4+} to Ce^{3+}.[37,38] Hence, the location of the Ce^{3+} ion is a new variable that needs to be explored in order to find the global minimum of the H/CeO_2(111) system—a lesson that has been learned from investigations of near-surface oxygen vacancies on CeO_2(111); Ce^{3+} ions prefer next-nearest neighbor sites to the vacancies and rather in the outermost Ce-layer.[56,57,61–63]

For consistency with previous theoretical calculations, we have also checked the adsorption of H on top of a Ce^{4+} ion in the second atomic layer of a (2×2) unit cell. Our results confirm that this is a very unfavorable adsorption site (adsorption energy 3.42 eV larger than on the O_{surf} site), and that no electron is transferred to the ceria surface. We have also studied the effect of the H coverage (θ = 1/16, 1/9, and 1/4 H ML), considering adsorption on O_{surf} sites and allowing for two different locations of the Ce^{3+} ion, namely, nearest and next-nearest neighbor (H-NN and H-NNN, respectively) to the OH group: the relaxed geometries at θ = 1/16 are illustrated in Fig. 2 and the computed binding energies as a function of H coverage are given in Table I. We note that the binding energies for an isolated species at θ = 1/16 and 1/9 are very similar, and that the adsorption energy is essentially independent on the location of Ce^{3+} ions. For such low H concentrations (i.e., large unit cells), the system is able to easily relax the lattice strain induced by the more spacious Ce^{3+} ion compared to its Ce^{4+} ion counterpart. These results compare well with those reported in Ref. 38 for θ = 1/9 using a very similar computational setup. However, Penschke *et al.*[59]

reported a value which is by ∼0.1 eV lower for the H-NNN configuration and $\theta = 1/16$. The use of a higher plane-wave cutoff (600 eV) might explain the difference with our results. Upon increasing coverage up to 1/4 ML, the binding for the H-NN configuration may suggest that 1/16 > 1/9 > 1/4, but at higher 1/4 coverage, the H-NNN configuration is 0.14 eV more stable than H-NN.[60] In addition, we notice that the O atoms of OH groups protrude ∼0.4 Å with respect to the average position of the rest of O_{surf} atoms. Hence, as θ increases from 1/16 to 1/4, counteracting lattice relaxation effects induced by the H adsorption and the localization of the charge transferred are likely to render the Ce nearest neighbor position to the OH group somewhat less stable than the next-nearest one for the Ce^{3+} species at the higher concentrations.

We discuss now the adsorption of nearest neighbor pairs (2H–O_{close}, O–O distance ∼3.9 Å) and trimers (3H) on CeO_2(111). These pairs have been modeled employing (4×4), (3×3), (2×2), and ($\sqrt{3}$×1) cells, whereas trimers the (4×4) cell. In addition, for the 2H structure with (4×4), next-nearest neighbor pairs (2H–O_{far}, O–O distance ∼6.7 Å) have been considered (Fig. 2). In all cases, several configurations for the Ce^{3+} ions have been examined. We limit the discussion to high-spin states because the difference between these states and any other spin state is less than 0.01 eV. Inspection of the results (Table I), reveals that the 2H–O_{close} and 2H–O_{far} structures with (4×4) periodicity are comparable in their stability. As the concentration of 2H–O_{close} pairs increases while decreasing the cell size from (4×4) to (3×3), the corresponding adsorption energy does not noticeably change. A 2H–O_{close} pair is energetically preferred by 0.07 eV/H than 2 isolated H atoms. In line with the case of isolated H atoms discussed above, a further coverage increase (from (3×3) to (2×2), and $\sqrt{3}$×1) is accompanied by effective repulsive interactions resulting in a net binding energy decrease. Our results for the two smaller cells compare well with that of Watkins *et al.*[29,64] for a (2×$\sqrt{2}$) cell with PW91+U (U = 5 eV) (once the same energy reference is used, i.e., free H atom instead of $\frac{1}{2}H_2$). However, Chen *et al.*[28] using PW91+U (U = 6.3 eV) and a ($\sqrt{3}$×1) cell obtained a value of −1.40 eV/atom (Table I). Using the same XC functional and U value, we have found this binding energy to be ∼0.2 eV larger, independently of the slab thickness. We note now, and discussed below, that the outward relaxation of the O_{surf} atoms belonging to neighboring OH groups is larger than that for isolated species.

Motivated by the already mentioned scanning probe microscopy studies of the hydroxilated surfaces,[13,19] where triangular-shaped triple protrusions have been associated to OH groups, corresponding 3H structures with H atoms chemisorbed on nearest-neighbor O_{surf} atoms have been investigated. We have considered two different structures, where the triangles are centered either on a O_{sub} or on a Ce^{4+} ion in the second atomic layer (Figs. 2 and 3, structures labeled 3H–O_{close}–O and 3H–O_{close}–Ce, respectively). The result of the thorough inspection of possible configurations for the 3 Ce^{3+} ions in the outermost Ce layer is shown in Table II. The most stable trimer is of the 3H–O_{close}–O type with Ce^{3+} ions in NN positions to the OH groups; it is by ∼0.15 eV more stable than three isolated H atoms (Table I). This result is consistent with the observed preference for H trimers instead of H pairs or scattered single H atoms. Figure 2 clearly shows that the atomic distortions induced by H adsorption on nearest neighbor O_{surf} sites, which are accompanied by the localization of the transferred charge, are cumulative: the upward displacement of the O_{surf} atoms where the H are located

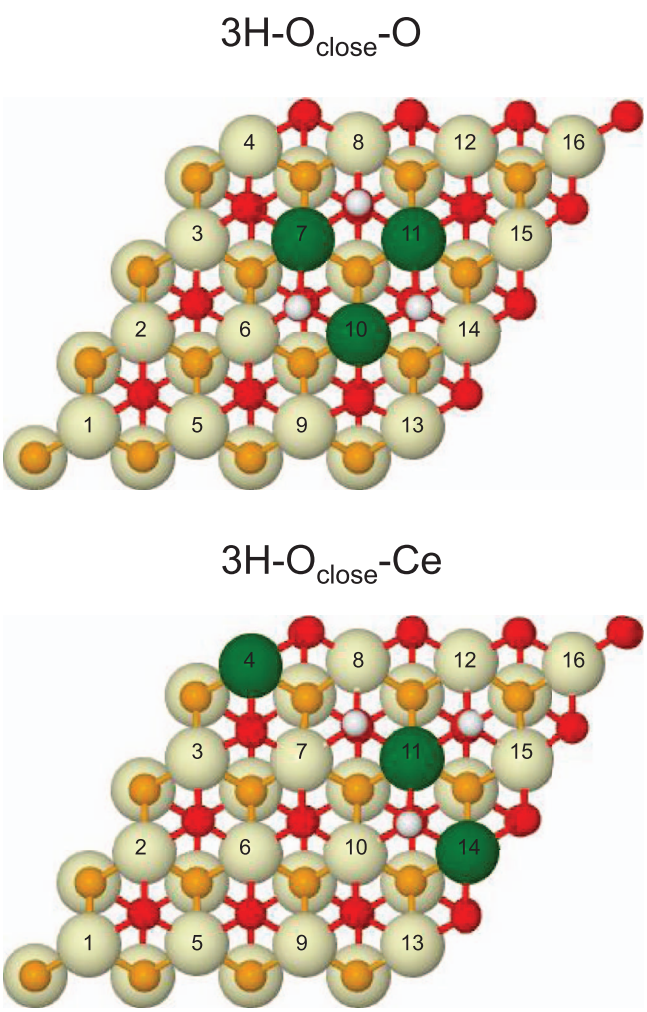

FIG. 3. Most stable 3H–O_{close}–O (7–10–11) and 3H–O_{close}–Ce (4–11–14) structures. Labels of the different locations for the Ce^{3+} ions are indicated. Color code as Fig. 2.

TABLE II. Binding energies (with respect to $\frac{1}{2}H_2$ in eV/H) for OH trimers (three H atoms chemisorbed on O_{surf} atoms forming a triangle) centered either on a O_{sub} (3H–O_{close}–O) or on a Ce^{4+} ion (3H–O_{close}–Ce) for different Ce^{3+} configurations. The atom numbers correspond to those in Figure 3.

3H–O_{close}–O		3H–O_{close}–Ce	
Ce^{3+}	E	Ce^{3+}	E
07–10–11	−1.22	04–11–14	−1.19
07–10–14	−1.19	07–11–15	−1.19
07–08–14	−1.14	10–11–14	−1.19
06–07–08	−1.12	08–10–15	−1.14
08–09–14	−1.07	04–14–15	−1.07
08–03–15	−1.05	04–13–16	−1.05
08–09–13	−1.05	...	...

gradually increases by up to 0.07 Å as H clusters of 1–3 atoms form. The stability of the H trimer and its large normal displacement provide an explanation for the frequent experimental observation by nc-AFM and STM of bright spots on three neighboring O_{surf} atoms and would be consistent with the assignment of this feature to a triple hydroxyl defect.[13,19]

V. H_2 ACTIVATION ON CLEAN AND REDUCED CeO_2(111) SURFACES

In Secs. III–IV we have characterized the initial and final steps of H_2 dissociation: the molecular and dissociative adsorption of H_2. Now, we explore the reaction mechanism and energy barrier of this process. This has been already addressed by Chen *et al.*,[28] that reported an energy barrier of 0.22 eV calculated on a $(\sqrt{3}\times1)$ cell. We have carefully revisited this study. Although the coordinates of the atoms in the transition structure were not provided, we have inspected the structural models in their figures and constructed a model for their transition state (TS) structure and performed a CI-NEB calculation, including the TS structure as one of the images, using the same computational setup. Our results show that the proposed structure does not correspond to a transition state and the CI-NEB calculation converges to a quite different structure. This fundamental discrepancy with the published results prompted us to perform a systematic analysis of the dissociation process, considering different initial (H_2–O_{surf} and H_2–Ce) and final structures (a few 2H–O_{close} structures, including the global minimum in Fig. 2). We have also addressed the influence of H coverage in the mechanism, using different unit cells, i.e., (3×3), (2×2), and $(\sqrt{3}\times1)$; for the smallest$(\sqrt{3}\times1)$ cell, we have tested both PBE+U(4.5 eV) and PW91+U(6.3 eV).

We found that the homolytic bond dissociation process is actually quite complex involving an heterolytic-like transition structure along the path. We started the search of the minimum energy pathway (MEP) connecting two local minima (cf. Fig. 2), namely, the H_2–Ce molecular adsorption as the initial state, and the 2H–O_{close} as the final state (cf. the first and last panels in Fig. 4) with a (3×3) unit cell. We tried different approaches (NEB, CI-NEB) with different parameters (e.g., spring constants, 5–7 images) but, in all of the cases, proper convergency to the MEP could not be achieved—a hint to the complexity of the path. However, we managed to identify among the resulting images, a particularly stable structure (second panel in Fig. 4), which we have actually characterized by vibrational analysis as a shallow local energy minimum (LEM-diss). This structure lies 0.76 (0.77) eV above the molecular adsorption state in the (3×3) [(2×2)] unit cell (Table I). In this structure, the H_2 molecule has moved from the Ce adsorption site toward one of the neighboring O_{surf} atoms, which protrudes 0.17 Å with respect to the O_{surf} average height, breaking the symmetry of the initial configuration and approaching the ceria surface. This structure is characterized by a stronger interaction with the surface atoms and a weaker molecular bond. The distance between the protruding O_{surf} and the closest H atom in the stretched molecule is 1.15 Å, already close to the final distance of 0.98 Å in the 2H–O_{close} final state; the H–H distance has increased to 1.12 Å, from the 0.75 Å distance in the free molecule. The closest Ce–H distances are 2.26 and 2.42 Å (2.87 Å in the initial state).

In order to fully characterized the dissociation process and determine the energy barrier, we have taken the above-mentioned local minimum structure (LEM-diss), and run two CI-NEB calculations with 5 images each, and start/end points at the local minima of the initial path. The converged results for the two CI-NEB calculations are displayed together in Fig. 5 (blue line). They show that the dissociation process involves three different steps. First, there is a weakening of the molecular bond, induced by the larger surface-molecule interaction as the molecule approaches to the surface, resulting in the local energy minimum already discussed. From this point, the H–H separation increases, leading the system to a transition state (TS-diss) where one of the H atoms is attached to a O_{surf} and the other one sits on a Ce site (third panel in Fig. 4); in the TS structure, therefore, only one Ce^{3+} is formed. This TS-diss structure lies 0.99 eV above the molecular adsorption state. Finally, the H atom is transferred from the Ce site to a

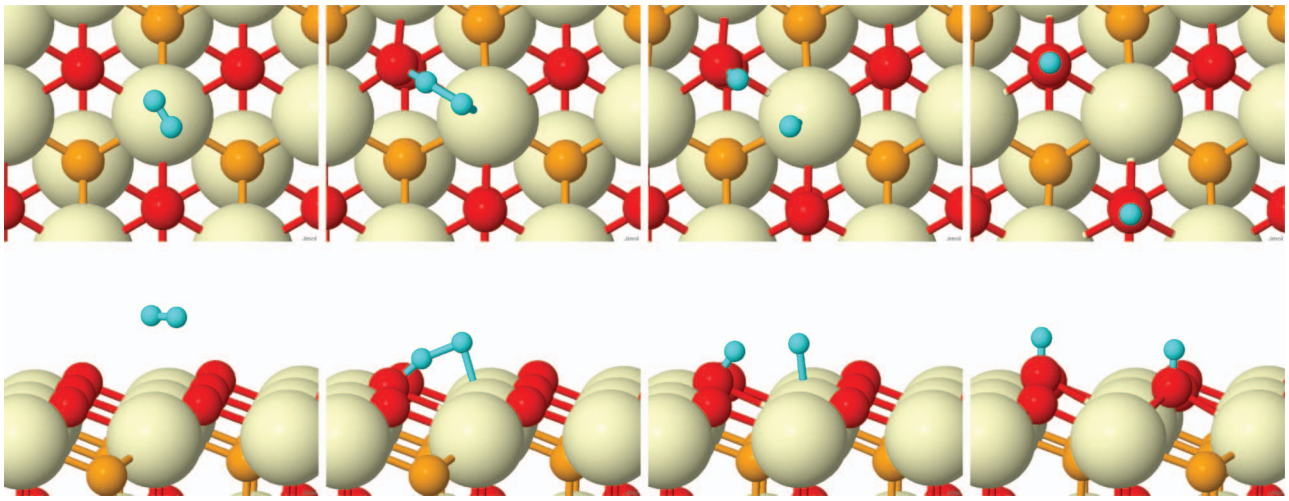

FIG. 4. Atomistic mechanism for the molecular dissociation. The ball-and-stick structures represent the top and side views of the initial configuration, the local minimum (LEM-diss), the transition state (TS-diss), and the final dissociated state found in the CI-NEB calculations for the 3×3 unit cell. Color code as Fig. 2.

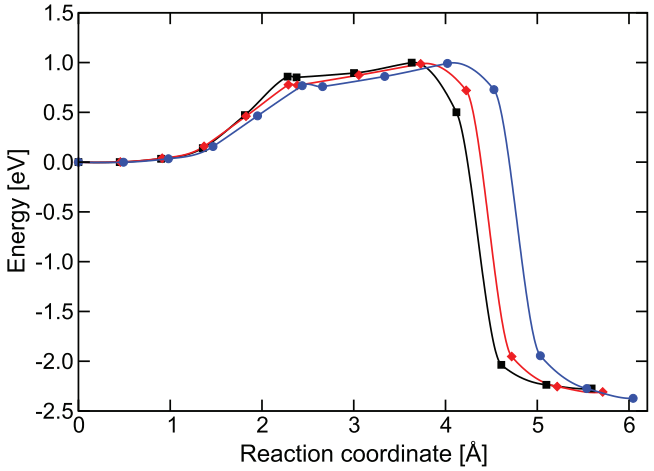

FIG. 5. Minimum energy path (MEP) for H_2 dissociation on the clean $CeO_2(111)$ surface for three different unit cells: 3×3 (blue), 2×2 (red), and $\sqrt{3}\times1$ (black). The MEP combines two independent CI-NEB calculations with 5 images: (i) from the initial configuration to the local energy minimum (LEM-diss), and (ii) from the LEM-diss, through the transition state (TS-diss), to the final dissociated configuration. The circles represent the energy of the images (taken the molecular adsorption state as the reference) and the lines correspond to splines interpolating these values.

neighboring H site, completing a full homolytic dissociation process of both H atoms. This last step is accompanied by the reduction of an additional Ce^{4+} ion.

In addition, we have also considered the dissociation process in the (2×2), and ($\sqrt{3}\times1$) cells (cf., Fig. 5 and Table I). H_2 dissociation follows the same three steps already identified in the (3×3) cell. In fact, the minimum energy paths for the (2×2) and (3×3) are almost identical. In the ($\sqrt{3}\times1$) cell, the intermediate LEM-diss structure lies 0.09 eV higher than in the (3×3) cell, but the energy of the TS-diss structure is essentially the same (1.00 eV). This high energy barrier is in direct conflict with the low activation energy (0.22 eV) reported by Chen *et al.*[28] We have not been able to reproduce their transition state structure and low activation energy even using similar computational details [($\sqrt{3}\times1$) cell and PW91+U(6.3 eV)]. Instead, our PW91+U(6.3 eV) calculations show the same local energy minimum identified with PBE+U(4.5 eV), lying 0.84 eV higher than the adsorbed H_2 molecule (cf., Fig. 5 and Table I). In contrast to the PBE+U(4.5 eV) result, the PW91+U(6.3 eV) energy path toward the second stage in the dissociation is almost flat, leading to very little change in the final barrier (0.85 eV).

In summary, our calculations with different functionals and surface periodicities –including the ones used by Chen *et al.*[28] – produce consistently a large (∼1.0 eV) energy barrier for H_2 dissociation on $CeO_2(111)$. This large value is, for example, more consistent with recent experimental observations, where a high temperature (523 K) and a large H_2/C_2H_2 = 30 ratio is required to achieve maximum conversion efficiency for acetylene hydrogenation.[27]

Finally, we investigate whether the presence of an oxygen vacancy on $CeO_2(111)$ has any effect on the dissociation of the hydrogen molecule. For this study we have chosen a (2×2) cell with a surface oxygen vacancy. The corresponding global minimum for this defect structure is illustrated in Fig. 1(b).

TABLE III. Binding energies (in eV/H_2 and with respect to $\frac{1}{2}H_2$ in eV/H) for the different steps of H_2 dissociation over Ce^{3+} and Ce^{4+} sites on $CeO_2(111)$ with a surface oxygen vacancy and (2 × 2) periodicity. The equivalent energies on the corresponding clean $CeO_2(111)$ are also shown for comparison.

Site	H_2–Ce	2H–O_{close}	TS-diss
Ce^{4+}	−0.05	−0.88	0.90
Ce^{3+}	−0.04	−0.88	1.10
Ce^{4+} (clean)	−0.03	−1.17	1.00

The two Ce^{3+} ions are located in the third and fifth atomic layer, respectively.[56,57] Hence, the structure has two kinds of surface cerium ions: one Ce^{3+} ion located in a next-nearest neighbor position with respect to the vacancy, and three equivalent Ce^{4+} ions which are surrounding the vacancy in nearest-neighbor positions. We have studied the dissociation process considering the H_2–Ce initial molecular adsorption state on these two inequivalent Ce ions. Our results for the energy of the initial, final, and transition state structures are collected in Table III. For the adsorbed H_2 molecule there is no significant change in the binding energy. However, the final dissociated state, 2H–O_{close}, is about ∼0.6 eV less stable near both kinds of ions compared to the clean surface. This is related to the need to accommodate the strain created by four different Ce^{3+} ions on this relatively small unit cell. The dissociation process follows the same three steps discussed above for the clean surface, with a similar transition state structure and a reaction barrier ∼0.1 eV smaller (larger) when the molecule is initially adsorbed on a Ce^{4+} (Ce^{3+}) ion. These findings would not explain the already mentioned detrimental effect of O_{surf} vacancies to the conversion of alkynes to olefins;[27] it is likely associated with the reduction of the available O_{surf} sites for the adsorption of the reactants.[41]

VI. DIFFUSION OF H ATOMS ON CLEAN $CeO_2(111)$

We discuss now H atom diffusion over $CeO_2(111)$ surface, a process that may occur upon, for example, H_2 dissociation. To study this process, we have considered a single H atom chemisorbed on a (3×3) cell of clean $CeO_2(111)$, with the Ce^{3+} ion located in a next-nearest-neighbor configuration (H-NNN in Fig. 2). We have tested several different paths connecting this initial structure and its equivalent translations. We have found that the lowest-energy path goes through a local adsorption minimum structure discussed in Sec. IV, where atomic H is chemisorbed on the O_{sub} in the third layer instead of O_{surf} and is by ∼1.6 eV less stable than H-NNN. The results of a CI-NEB calculation with 5 images for the first half of the reaction process, where the H atom moves from an O_{surf} (initial state) to the local adsorption minimum on top of an O_{sub} are shown in Fig. 6. In the transition state structure, (TS-diff, Fig. 6), the hydrogen atom is already closer to the O_{sub} atom but still shared with the O_{surf} as shown by the stretched O–H bonds of ∼1.16 and 1.36 Å, respectively. From here, the system quickly evolves to the final adsorption configuration on top of the O_{sub} atom, with an O_{sub}–H bond distance of 0.98 Å. The energy barrier for diffusion is ∼1.8 eV, referred to H-NNN. The second part of the process, where the

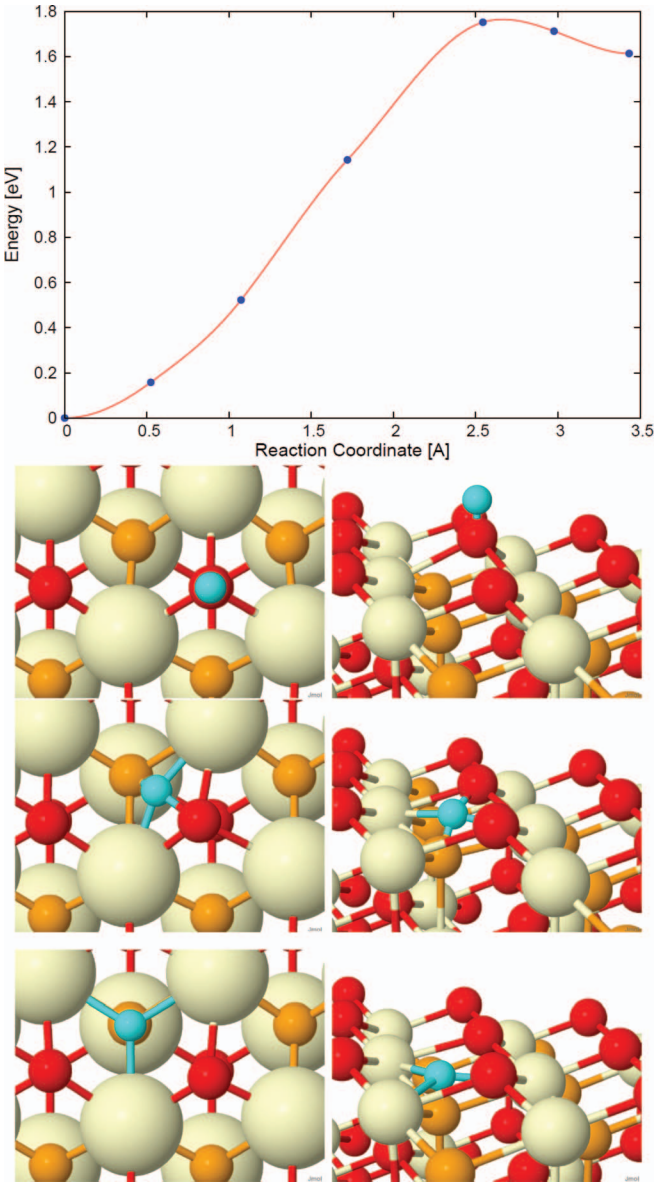

FIG. 6. Minimum energy path for H diffusion over $CeO_2(111)$ [(3×3)]. (Top) CI-NEB results for the first half of the reaction process, where the H atom moves from an O_{surf} (initial state) to the local adsorption minimum on top of an O_{sub} in the third layer. The second part of the process, where the H atom moves from the O_{sub} to a neighboring O_{surf} is completely equivalent. (Bottom) Initial, transition (TS-diff) and final state structures. Color code as Fig. 2.

H atom moves from the O_{sub} to a neighboring O_{surf} is completely equivalent.

VII. CONCLUSIONS

We have presented a detailed DFT+U study of the mechanisms underlaying the dissociation of molecular hydrogen and the diffusion of the resulting atomic species on $CeO_2(111)$ surfaces. The hydrogen molecule is physisorbed on the surface, with a global minimum where the H_2 lies flat on top of a Ce^{4+} and a very flat potential energy surface that allows the molecule to rotate and diffuse almost freely. van der Waals interactions between H_2 and ceria are small, increasing the molecular adsorption energy by ∼50 meV, without changing the relative stability of the adsorption sites.

The adsorption of isolated H species on an O_{surf} atom is an exothermic process, with a chemisorption energy of ∼1.2 eV, and leads to an upwards O_{surf} displacement of ∼0.4 Å with the transfer of one electron driving the $Ce^{4+}\rightarrow Ce^{3+}$ reduction. We have explored how several factors, including H coverage, the Ce^{3+} location, and the U value, affect the chemisorption energy. Furthermore, we have considered the formation of pairs and trimer H aggregates. Our results show that at low H coverages, triangular-shaped trimers centered around a O_{sub} in the third atomic layer, with the three Ce^{3+} ions neighboring the OH groups, are energetically favorable. The distortions induced by the H adsorption, which are accompanied by the formation of the larger Ce^{3+} ions in the outermost cerium layer, are cumulative with a total upward relaxation of ∼0.5 Å. The trimer stability and its normal displacement provide an explanation for the frequent experimental observation by nc-AFM and STM of bright spots on three neighboring O_{surf} atoms and supports the assignment of this feature to a triple hydroxyl defect.

Our comprehensive study of the reaction mechanism that includes varying the H coverage (i.e., the cell size) and the methodology [PBE+U(4.5 eV), PW91+U(6.3 eV)], shows conclusively that the H_2 dissociation is an activated process with an energy barrier of ∼1.0 eV, which is not significantly affected by coverage or the presence of surface oxygen vacancies. This value, significantly larger than a previous theoretical prediction, is consistent with recent experimental results that point out to dissociation as the rate-limiting step in the high selective partial hydrogenation of alkynes on ceria substrates.[27,41] Interestingly, the reaction proceeds through a local energy minimum where the molecule is located close to one of the surface oxygen atoms and the H–H bond has been substantially weaken by the interaction with the substrate. The transition state structure connecting this local energy minimum with the final state involves H–Ce and H–O_{surf} bonds, where one of the two electrons of the initial H_2 molecule is transferred to the ceria surface, while the other one remains with the H attached to the Ce atom.

The path for the diffusion of H atoms on the surface goes through the adsorption on-top of the oxygen in the third atomic layer with a barrier of ∼1.8 eV. Such a large barrier, supports the presence of excess H as the key factor in the observed high selectivity. For instance, in the hydrogenation of acetylene, H atoms block the coupling of ethylene with C_2H_3 species preventing oligomer formation.[41] Fundamental understanding of the H_2 dissociation on ceria surfaces is paramount for the interpretation of the chemical reactions involving hydroxyl intermediates on ceria-based catalysts. Clearly, both large activation barriers for H_2 dissociation and H diffusion cannot be ignored when considering reaction mechanisms.

Note added in proof: We have just become aware of a recent publication by García-Melchor and Lopez[65] where a 1.08 eV barrier for H2 dissociation on $CeO_2(111)$ is predicted.

ACKNOWLEDGMENTS

We thank MINECO (CTQ2012-32928, PLE2009-0061, MAT2011-23627, and CSD2010-00024) for financial

support. Computer time provided by the SGAI-CSIC, CESGA, BIFI-ZCAM, University of Cantabria-IFCA, and the BSC (through the Spanish Supercomputer Network, RES) is acknowledged. This work was granted access HPC resources made available within the Distributed European Computing Initiative by the PRACE-2IP, receiving funding from the EU's FP7 Programme under Grant Agreement No. RI-283493. J.C. is supported by the MINECO through a Ramón y Cajal Fellowship and acknowledges support by the Marie Curie Career Integration Grant FP7-PEOPLE-2011-CIG: Project NanoWGS and The Royal Society through the Newton Alumnus scheme. The COST action CM1104 is gratefully acknowledged.

[1]A. Trovarelli, C. de Leitenburg, M. Boaro, and G. Dolcetti, Catal. Today **50**, 353 (1999).
[2]Z. Shao and S. M. Haile, Nature (London) **431**, 170 (2004).
[3]A. S. Karakoti, S. Singh, A. Kumar, M. Malinska, S. V. N. T. Kuchibhatla, K. Wozniak, W. T. Self, and S. Seal, J. Am. Chem. Soc. **131**, 14144 (2009).
[4]Q. Fu, H. Saltsburg, and M. Flytzani-Stephanopoulos, Science **301**, 935 (2003).
[5]S. Hilaire, X. Wang, T. Luo, R. Gorte, and J. Wagner, Appl. Catal., A **215**, 271 (2001).
[6]O. Pozdnyakova, D. Teschner, A. Wootsch, J. Kröhnert, B. Steinhauer, H. Sauer, L. Toth, F. Jentoft, A. Knop-Gericke, Z. Paál, and R. Schlögl, J. Catal. **237**, 1 (2006).
[7]M. Boaro, M. Vicario, C. de Leitenburg, G. Dolcetti, and A. Trovarelli, Catal. Today **77**, 407 (2003).
[8]E. Aneggi, M. Boaro, C. de Leitenburg, G. Dolcetti, and A. Trovarelli, J. Alloys Compd. **408–412**, 1096 (2006).
[9]B. Chen, Y. Ma, L. Ding, L. Xu, Z. Wu, Q. Yuan, and W. Huang, J. Phys. Chem. C **117**, 5800 (2013).
[10]L. Kundakovic, D. Mullins, and S. Overbury, Surf. Sci. **457**, 51 (2000).
[11]M. Henderson, C. Perkins, M. Engelhard, S. Thevuthasan, and C. Peden, Surf. Sci. **526**, 1 (2003).
[12]S. Gritschneder, Y. Iwasawa, and M. Reichling, Nanotechnology **18**, 044025 (2007).
[13]S. Gritschneder and M. Reichling, Nanotechnology **18**, 044024 (2007).
[14]X. Zhao, S. Ma, J. Hrbek, and J. A. Rodriguez, Surf. Sci. **601**, 2445 (2007).
[15]S. D. Senanayake, D. Stacchiola, J. Evans, M. Estrella, L. Barrio, M. Pérez, J. Hrbek, and J. A. Rodriguez, J. Catal. **271**, 392 (2010).
[16]D. R. Mullins, P. M. Albrecht, T.-L. Chen, F. C. Calaza, M. D. Biegalski, H. M. Christen, and S. H. Overbury, J. Phys. Chem. C **116**, 19419 (2012).
[17]V. Matolín, I. Matolínová, F. Dvorak, V. Johnek, J. Myslivecek, K. Prince, T. Skála, O. Stetsovych, N. Tsud, M. Vaclavu, and B. Smid, Catal. Today **181**, 124 (2012).
[18]Y. Lykhach, V. Johánek, H. A. Aleksandrov, S. M. Kozlov, M. Happel, T. Skála, P. S. Petkov, N. Tsud, G. N. Vayssilov, K. C. Prince, K. M. Neyman, V. Matolín, and J. Libuda, J. Phys. Chem. C **116**, 12103 (2012).
[19]D. C. Grinter, R. Ithnin, C. L. Pang, and G. Thornton, J. Phys. Chem. C **114**, 17036 (2010).
[20]J. Paier, C. Penschke, and J. Sauer, Chem. Rev. **113**, 3949 (2013).
[21]S. Kumar and P. K. Schelling, J. Chem. Phys. **125**, 204704 (2006).
[22]W. O. Gordon, Y. Xu, D. R. Mullins, and S. H. Overbury, Phys. Chem. Chem. Phys. **11**, 11171 (2009).
[23]A. Joshi, A. Rammohan, Y. Jiang, and S. Ogunwumi, J. Mol. Struct. **912**, 73 (2009).
[24]Y. Segura, N. López, and J. Pérez-Ramírez, J. Catal. **247**, 383 (2007).
[25]Y. Azizi, C. Petit, and V. Pitchon, J. Catal. **256**, 338 (2008).
[26]Y. Guan and E. J. M. Hensen, Phys. Chem. Chem. Phys. **11**, 9578 (2009).
[27]G. Vilé, B. Bridier, J. Wichert, and J. Pérez-Ramírez, Angew. Chem. Int. Ed. **51**, 8620 (2012).
[28]H.-T. Chen, Y. M. Choi, M. Liu, and M. C. Lin, Chem. Phys. Chem. **8**, 849 (2007).
[29]M. B. Watkins, A. S. Foster, and A. L. Shluger, J. Phys. Chem. C **111**, 15337 (2007).
[30]M. Fronzi, S. Piccinin, B. Delley, E. Traversa, and C. Stampfl, Phys. Chem. Chem. Phys. **11**, 9188 (2009).
[31]Z. Yang, Q. Wang, S. Wei, D. Ma, and Q. Sun, J. Phys. Chem. C **114**, 14891 (2010).
[32]D. Marrocchelli and B. Yildiz, J. Phys. Chem. C **116**, 2411 (2012).
[33]M. Molinari, S. C. Parker, D. C. Sayle, and M. S. Islam, J. Phys. Chem. C **116**, 7073 (2012).
[34]S. Fuente, M. M. Branda, and F. Illas, Theor. Chem. Acc. **131**, 1190 (2012).
[35]D. Fernández-Torre, K. Kośmider, J. Carrasco, M. V. Ganduglia-Pirovano, and R. Pérez, J. Phys. Chem. C **116**, 13584 (2012).
[36]Z. Chafi, N. Keghouche, and C. Minot, in *Proceedings of the JMSM 2008 Conference* [Phys. Proc. **2**, 673 (2009)].
[37]G. Vicario, G. Balducci, S. Fabris, S. de Gironcoli, and S. Baroni, J. Phys. Chem. B **110**, 19380 (2006).
[38]C. Popa, M. V. Ganduglia-Pirovano, and J. Sauer, J. Phys. Chem. C **115**, 7399 (2011).
[39]J. P. Perdew, J. A. Chevary, S. H. Vosko, K. A. Jackson, M. R. Pederson, D. J. Singh, and C. Fiolhais, Phys. Rev. B **46**, 6671 (1992).
[40]J. Perdew, K. Burke, and M. Ernzerhof, Phys. Rev. Lett. **77**, 3865 (1996).
[41]J. Carrasco, G. Vilé, D. Fernádez-Torre, R. Pérez, J. Pérez-Ramírez, and M. V. Ganduglia-Pirovano, J. Phys. Chem. C **118**, 5352 (2014).
[42]S. Dudarev, G. Botton, S. Savrasov, C. Humphreys, and A. Sutton, Phys. Rev. B **57**, 1505 (1998).
[43]G. Kresse and J. Furthmüller, Comput. Mater. Sci. **6**, 15 (1996).
[44]G. Kresse and J. Furthmüller, Phys. Rev. B **54**, 11169 (1996).
[45]S. Fabris, S. de Gironcoli, S. Baroni, G. Vicario, and G. Balducci, Phys. Rev. B **71**, 041102 (2005).
[46]M. Cococcioni and S. de Gironcoli, Phys. Rev. B **71**, 035105 (2005).
[47]C. W. M. Castleton, J. Kullgren, and K. Hermansson, J. Chem. Phys. **127**, 244704 (2007).
[48]J. Klimeš, D. R. Bowler, and A. Michaelides, Phys. Rev. B **83**, 195131 (2011).
[49]M. Dion, H. Rydberg, E. Schröder, D. Langreth, and B. Lundqvist, Phys. Rev. Lett. **92**, 246401 (2004).
[50]J. P. Prates Ramalho, J. R. B. Gomes, and F. Illas, RSC Adv. **3**, 13085 (2013).
[51]J. Klimeš and A. Michaelides, J. Chem. Phys. **137**, 120901 (2012).
[52]W. Liu, V. G. Ruiz, G.-X. Zhang, X. R. Biswajit Santra, M. Scheffler, and A. Tkatchenko, New J. Phys. **15**, 053046 (2013).
[53]W. Liu, J. Carrasco, B. Santra, A. Michaelides, M. Scheffler, and A. Tkatchenko, Phys. Rev. B **86**, 245405 (2012).
[54]H. Yildirim, T. Greber, and A. Kara, J. Phys. Chem. C **117**, 20572 (2013).
[55]J. Carrasco, W. Liu, A. Michaelides, and A. Tkatchenko, J. Chem. Phys. **140**, 084704 (2014).
[56]M. V. Ganduglia-Pirovano, J. L. F. Da Silva, and J. Sauer, Phys. Rev. Lett. **102**, 026101 (2009).
[57]G. E. Murgida and M. V. Ganduglia-Pirovano, Phys. Rev. Lett. **110**, 246101 (2013).
[58]G. Henkelman, B. Uberuaga, and H. Jonsson, J. Chem. Phys. **113**, 9901 (2000).
[59]C. Penschke, J. Paier, and J. Sauer, J. Phys. Chem. C **117**, 5274 (2013).
[60]M. V. Ganduglia-Pirovano, C. Popa, J. Sauer, H. Abbott, A. Uhl, M. Baron, D. Stacchiola, O. Bodarchuk, S. Shaikhutdinov, and H.-J. Freund, J. Am. Chem. Soc. **132**, 2345 (2010).
[61]H.-Y. Li, H.-F. Wang, X.-Q. Gong, Y.-L. Guo, Y. Guo, G. Lu, and P. Hu, Phys. Rev. B **79**, 193401 (2009).
[62]J.-F. Jerratsch, X. Shao, N. Nilius, H.-J. Freund, C. Popa, M. V. Ganduglia-Pirovano, A. M. Burow, and J. Sauer, Phys. Rev. Lett. **106**, 246801 (2011).
[63]J. J. Plata, A. M. Márquez, and J. F. Sanz, J. Phys. Chem. C **117**, 25497 (2013).
[64]M. Watkins, personal communication (2013).
[65]M. García-Melchor, and N. López, J. Phys. Chem. C **118**(20), 10921 (2014).